PCCP
Physical Chemistry Chemical Physics

Accepted Manuscript

This article can be cited before page numbers have been issued, to do this please use: A. Nelson, C. Ruby, E. André and D. Cornu, *Phys. Chem. Chem. Phys.*, 2026, DOI: 10.1039/D6CP00496B.

ROYAL SOCIETY OF CHEMISTRY

rsc.li/pccp

View Article Online
DOI: 10.1039/D6CP00496B

COMMUNICATION

Ab-initio molecular dynamics simulations evidence the templating role of cations in the green rust sulfate structure.

Adam Nelson[a], Christian Ruby[a], Erwan André[a], Damien Cornu[a]

Received 00th January 20xx,
Accepted 00th January 20xx

DOI: 10.1039/x0xx00000x

The intercalation of sodium into green rust sulfate, a layered double hydroxide (LDH), has been proposed to explain its large interlayer spacing (~11 Å). We compare structures with and without sodium using ab-initio molecular dynamics (AIMD) simulations and conclude that its composition most likely contains sodium: $Fe^{II}_6Fe^{III}_3(OH)_{18}Na(SO_4)_2{\cdot}nH2O$, with 14 ≤ n ≤ 16.

With positively charged layers and anions in the interlayer space, Layered Double Hydroxides are widely used for anionic exchange. However, adsorption of cations using this structure is possible, and can be explained by the co-insertion of cations with anions within the interlayer space.[1] The adsorption of cations is often associated with large anions with multiple negative charges, such as EDTA. However, the exchange of small monovalent cations (K^+, Na^+, Li^+) within sulfate intercalated LDH was experimentally proved in 2019.[2]

The incorporation of sodium within the structure is however still debated for Green Rust (GR). Green rust is a mixed-valence, Fe^{II}-Fe^{III} layered double hydroxide. It is an intermediate in the corrosion of steel to rust under specific conditions.[3,4] It has been shown to be a promising low-cost material for capturing and reducing polluting anions[5] (*ex:* AsO_4^{3-}, CrO_4^{2-}, NO_3^-) and compounds[6] in soils and groundwaters. When intercalated with tetrahedral anions, GR exhibits a distinct structure called hexagonal green rust or GR2, in opposition to the GR1 structure generated by halides or planar anions (CO_3^{2-}, SO_3^{2-}, Cl^-).[7,8] While the GR1 structure[9] is similar to that of pyroaurite ($Mg_6Fe_2CO_3(OH)_{16}.4H_2O$), that of GR2 is rarer among layered double hydroxides, with a large basal spacing (11.0 Å for GR2[10] vs 8.0 Å for some hydrotalcite sulfates)[11] and a hexagonal P-3 space group. This basal spacing can be found in other closely related compounds, like manganese sulfate LDHs,[12] motukoreaite[13] or green rust phosphates.[14]

For the incorporation of cations in the interlayer space, two conflicting descriptions of GR2 exist in the literature. Contributions prior to 2004[15–17] simply describe it as green rust sulfate ($Fe^{II}_8Fe^{III}_4(OH)_{24}(SO_4)_2{\cdot}nH_2O$), mirroring the standard formula of LDH compounds. However, these early studies[16,17] already detected an abnormally high amount of sodium in the compound and hypothesized its presence within the interlayer. Evidence collected from 2004 and onwards by Christiansen *et al.*[18,19] would push this hypothesis further and propose that sodium should be included in the stoichiometric formula of $GRSO_4$. Subsequent elemental analysis, Rietveld refinement and the substitution of Na^+ by other cations during the synthesis have offered multiple data points to support this hypothesis. However, more recent studies[20–22] and discussions[5,23–25] by other groups have not adopted this new description of green rust. As a result, two formulae can be found alternatively in recent publications: $Fe^{II}_8Fe^{III}_4(OH)_{24}(SO_4)_2{\cdot}nH_2O$ *vs* $Fe^{II}_6Fe^{III}_3(OH)_{18}Na(SO_4)_2{\cdot}nH_2O$. Part of the reticence to add sodium to the formula might be attributed to a lack of counterfactual evidence: although there is good evidence that GR2 can include cations in the interlayer, this does not exclude the possibility of a cation-free $GRSO_4$ or partially substituted $GRNaSO_4$ with similar structural parameters.

In addition to the presence or absence of the sodium cation, the reported hydration number also varies from one study to the next. A common number for the sodium-less formula is n = 16 (per *two* sulfate sites, corresponding to $Fe^{II}_8Fe^{III}_4(OH)_{24}(SO_4)_2{\cdot}16H_2O$), obtained by Simon *et al.*[15] through a combination of Rietveld analysis and DSC. Other values for n include ≈5-6 (from TGA),[26] and 4.[27] A commonly cited number for green rust sodium sulfate is n = 12 for 9 $Fe(OH)_2$ units,[10] which was to the best of our knowledge carried over from the formula for shigaite ($Al_3Mn_6(OH)_{18}(SO_4)_2Na{\cdot}12H_2O$), a similarly structured LDH.[28] Water content modifies the molecular weight of GR2 but also determines the mobility of the anion and the hypothetic cation in the interlayer space, affecting the speed of the anionic/cationic exchanges.

These uncertainties about the structure of GR2 are exacerbated by the experimental difficulties associated with the study of the compound. Despite being simple to synthesize from extremely accessible precursors, its analysis is complicated by its sensitivity to air. GR2 oxidizes rapidly in air, yielding iron(III) oxides in a few minutes of exposure, requiring anoxic conditions for any characterization. Because of its paramagnetic nature, solid state NMR observations would yield limited information due to fast transverse relaxation. XRD studies are also challenging, due to the the fluorescence effects induced by iron when using common copper anodes. Elemental analysis can also be misleading, due to the

[a] *Université de Lorraine, CNRS, LCPME, Nancy, F-54000, France.*

View Article Online
DOI: 10.1039/D6CP00496B

inability to distinguish cations adsorbed on the surface from interlayer sites.

Our study therefore seeks to use ab-initio simulations to determine which of the two descriptions of the GR2 structure best matches calculated parameters to experimental results. We therefore compare a sodium sulfate green rust ($GRNaSO_4$) of formula $Fe^{II}_6Fe^{III}_3(OH)_{18}Na(SO_4)_2{\cdot}nH_2O$ to a sulfate green rust with no cation in the interlayer ($GRSO_4$), of formula $Fe^{II}_8Fe^{III}_4(OH)_{24}(SO_4)_2{\cdot}nH_2O$, with n = 0-18

To study a wider range of configurations and account for dynamical effects, a molecular dynamics simulation in the NPT ensemble has been carried out for each of the structures. The aim of this study is to verify the plausibility of different descriptions of the interlayer and bring new arguments to resolve this long-standing ambiguity in the literature.

The green rust structures in this work were studied using first-principle Molecular Dynamics (MD) calculations. Firstly, a $GRNaSO_4$ structure ($Fe^{II}_6Fe^{III}_3(OH)_{18}Na(SO_4)_2{\cdot}12H_2O$) based on characterizations from the literature[10] was built and its structure refined through ionic relaxation. An alternate $GRSO_4$ structure was then built from the first, removing the Na^+ cation and expanding the $Fe(OH)_2$ layer to twelve sites, to achieve electroneutrality. The resulting structure ($Fe^{II}_8Fe^{III}_4(OH)_{24}(SO_4)_2{\cdot}12H_2O$) was relaxed in the same manner. The hydration number of the two structures was then altered by manually adding or removing water molecules (starting from a relaxed structure of the previous hydration number, and adding water in the largest interstice, or removing the water molecules with the weakest H-bonds), yielding green rusts with $n(H_2O)$ ranging from 0 to 18 for $GRSO_4$ and $GRNaSO_4$.

The GR structures were then refined using DFT (Density Functional Theory)[29,30] calculations in VASP,[31,32] firstly through ionic relaxation, then through an MD simulation. All calculations were carried out using the PAW method,[33] with a Perdew-Burke-Ernzerhof (PBE)[34] variation of the Generalized Gradient Approximation (GGA) of the energy functionals. These approximations have been widely used to study similar materials.[35,36] The electronic structure of Fe was corrected using the DFT+U framework,[37] with an U_{eff} value of 5.30 eV.[38] The cutoff energy of the planewave expansion was 400 eV, confirmed to be sufficient through convergence with respect to E_0 (Fig. S1). Dispersion forces were approximated using the Tkatchenko-Scheffler method.[39] The Brillouin zone integration used a 2*2*2 Monkhorst-Pack grid.[40] Additionally, the Fe ions were spin-polarized in the simulation, starting from an initial antiferromagnetic state.

The initial geometric optimizations used the conjugate-gradient method for energy minimization, reducing the atomic forces to below to below 10^{-4} eV/Å, with a self-consistency energy threshold of 10^{-5} eV. No symmetry was imposed, with both atomic positions and cell parameters varying freely. This was followed by an MD simulation in the NPT ensemble, between 10 and 30 ps long, with time-steps of 1 fs, using the same parameters as the DFT relaxation.

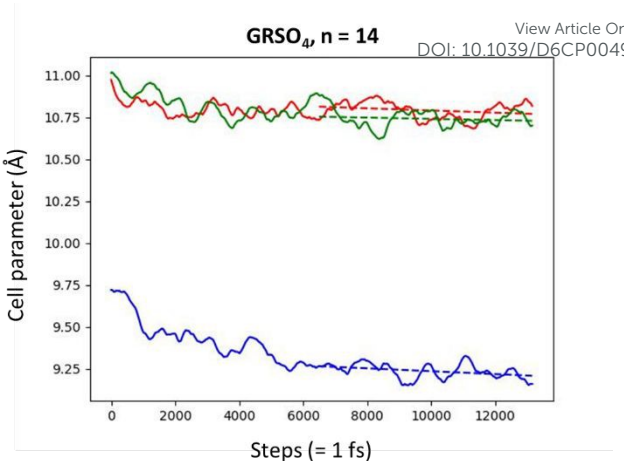

Fig. 1 Example evolution of the cell parameters over the length of the MD simulation, for $GRSO_4.14H_2O$. Note the initial stabilization period of ~6000 steps, followed by fluctuations around a near-equilibrium value. Only the second half of the MD is considered when calculating averaged crystallographic parameters. Red = a, green = b, blue = c. The trend lines are a linear fit of the cell parameters during the second half of the simulation.

A Parrinello-Rahman algorithm[41] was used to describe the system, which was coupled to a Langevin thermostat.[42] The temperature and external pressure were set to ambient conditions (1 bar, 297 K). The ion and lattice degrees of freedom were assigned a friction coefficient of 10 ps^{-1}. The fictitious mass of the lattice degrees of freedom was set at 5000 amu. The simulation was carried out until the cell parameters, pressure and temperature of the system were visually no longer showing a clear evolution in a single direction (see ex. in Fig. 1), then continued for at least the same duration (no less than 5 ps, up to 30 ps). Only the second part of the simulation (the production phase) was considered when calculating averaged structural parameters.

The data from the molecular dynamics simulations were then processed using a homemade Python program, using Numpy[43] for calculations and the MatPlotLib[44] module for plotting.

All MD simulations show an initial contraction of the cell, after which only relatively moderate fluctuations of the cell dimensions occur

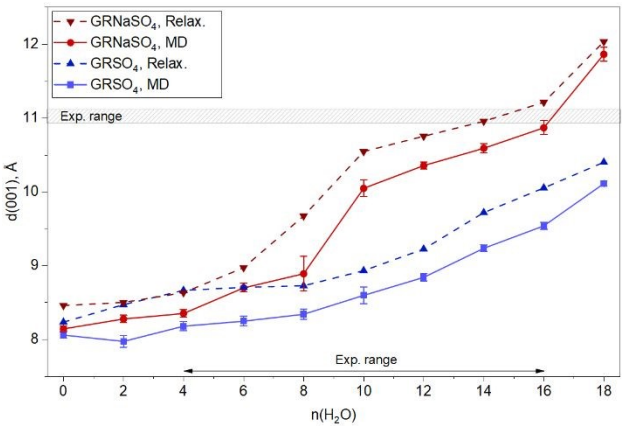

Fig. 2 Evolution of the d(001) distance for $GRSO_4$ and $GRNaSO_4$, as a function of the hydration number n. The error bars correspond to the mean deviation of the d(001) value over the length of the MD simulation.

Journal Name COMMUNICATION

(see Fig. 1, Fig. S2). This initial contraction compensates for an initial overestimation of the crystallographic parameters with respect to experimental measurements, leading to a slight underestimation (Tab. S1) over the length of the MD. This contraction can be explained by a weakening of the H-bond network induced by thermal agitation, evidenced by a reduction in the number of long-range H-bonds in the MD when compared to the 0 K structure (Fig. S3). During all of the MD simulations, the cell conserves a geometry close to the initial hexagonal cell shape over the simulation, with $\alpha = 120\pm1°$ and $\beta \approx \gamma = 90\pm6°$. The a and b cell parameters do not vary significantly as a function of the composition of the interlayer, with only the basal spacing showing significant differences. The strong fluctuation in basal spacing during the MD are explained by a weak dependence between free energy and interlayer spacing (Fig. S4, S5).

Our calculations of the averaged d(001) distance (Fig. 2) indicate that this distance varies strongly with the hydration number n. We therefore expect the interlayer spacing to be significantly affected by the hydration level. However, experimental measurements of this d(001) distance in GR2 via XRD are contained within 10.9 Å < d(001) < 11.15 Å.[41,42] The narrow range of these values for different studies and experimental conditions indicates that the interlayer spacing of GR2 shows little experimental variability. Therefore, this experimental fact can be understood with our calculation only if the compound has a stable hydration number.

The interlayer spacing is also significantly impacted by the presence of sodium in the structure. It is significantly higher for $GRNaSO_4$ than for $GRSO_4$ at hydration numbers of 6 and above. The experimental value of ≈ 11.0 is only reached for $GRNaSO_4$ with n = 14 (DFT) or n = 16 (MD). It may eventually be reached by $GRSO_4$, but would require a hydration number far above experimental measurements for the compound.

The difference in interlayer distance between the two structures can be explained by a templating effect of the cation on the water layers. LDHs with halides or small planar anions (ex: carbonate) typically only have a single water layer, while some LDHs with three-dimensional ions like SO_4^{2-} have a two-layer structure, which can be determined through XRD.[45] This was observed GR2, where Rietveld refinements have repeatedly evidenced[10,15] the presence of multiple water layers. Fig. 3 shows a projection of both structures along the b axis and the height of various atoms during the production phase of the MD. While sulfate groups in $GRSO_4$ sit at the same height, the sulfates at in $GRNaSO_4$ for n ≥ 10 have two distinct sites separated vertically by ≈ 2.0 Å. In both structures, the hydration layers align broadly with the height of the oxygens in the sulfate groups (Fig. 3). This leads to the outer water layers being ≈ 3.8 Å apart in $GRNaSO_4$ and ≈ 2.7 Å apart in $GRSO_4$ (n = 16), with $GRNaSO_4$ having additional minor layers in the middle of the interlayer space. The Na-O distance in our simulation is ≈ 2.3 Å (Fig. S6), which is slightly smaller than experimental distance measurements of the $[Na(H_2O)_6]^+$ complex in aqueous environments, reported to be $d_{(Na\text{-}O)} \approx 2.4$ Å.[46] Assuming a regular octahedron, the distance between two opposite faces would be $d_{(O\text{-}O)} \approx 3.5$ Å.

The distance between the outer water layers therefore closely matches the spacing imposed by the aquo-complex of sodium (3.3 vs 3.8 Å). The aquo complex of Na^+ is also attached to the hydroxyl layers through multiple stable H bonds ($d_{H\text{-}O}$ = 1.6 Å, see Fig. S7). Additionally, the SO_4^{2-} groups are indirectly linked to Na^+ through the water ligands by moderately stable H-bonds ($dS\text{-}O_{H2O} \approx 3.5$ Å, Fig. S8). This structured bonding between the sodium complex, the anions, the water layers and the layers is hypothesized to have a templating effect on the structure. This templating effect would stabilize the water layers. This could explain the non-linear increase in interlayer spacing with hydration (Fig. 2). This may also explain the narrow range of interlayer spacings measured in the literature, which stands in stark contrast to other sulfate LDHs that are highly susceptible to hydration conditions.[45]

We can confirm the accuracy of our simulated structure by comparing it to experimental results measured on closely related green rust structures. A strong experimental proof of the incorporation of cations in the GR2 interlayer has been offered by Christiansen *et al.* 2014,[19] where the sulfate green rust was synthesized in the presence of different alkali metals (Na^+, K^+, Rb^+, Cs^+) in order to measure differences in the d(001) distance through XRD measurements. It was demonstrated that the interlayer distance increased proportionally with the size of

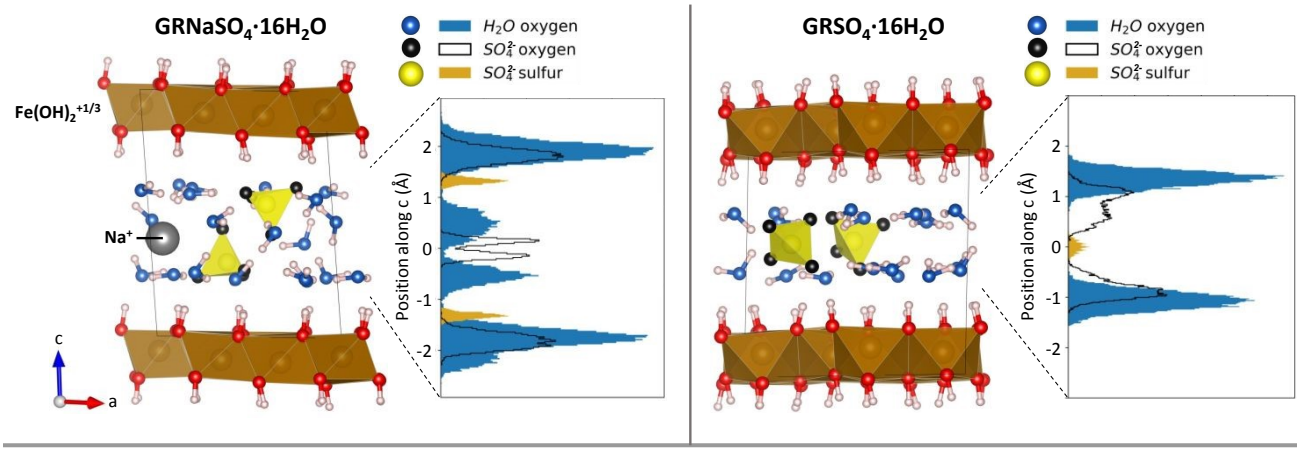

Fig. 3 Final frames of the MD simulations for $GRNaSO_4$ (left) and $GRSO_4$ (right), n = 16, inset with a histogram of the position along c of different atoms in the interlayer. Note the vertical separation of SO_4 sites in $GRNaSO_4$, not observed in $GRSO_4$. Also note the four hydration layers in $GRNaSO_4$. Visualization: VESTA.[47]

View Article Online
DOI: 10.1039/D5CP04058B

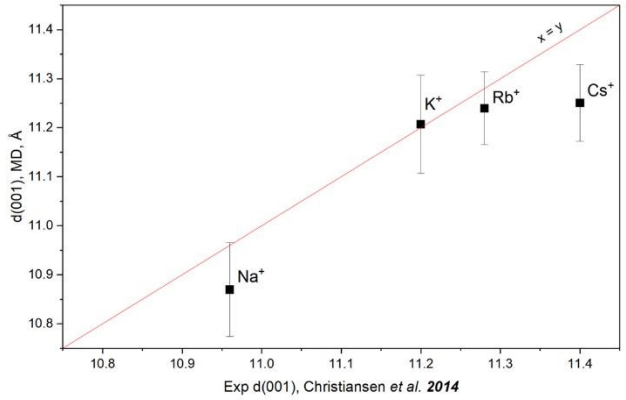

Fig. 4 DFT-calculated d(001) parameter as a function of experimental d(001) for different cation substitutions (Na^+, K^+, Rb^+, Cs^+) in the $GRNaSO_4$ structure. Experimental data from Christiansen *et al.*, 2014.[14] The red line indicates a perfect correspondence between theoretical and experimental distances

the metal cation. We therefore simulated the same $GRNaSO_4$ structure and applied MD, with Na^+ replaced with these larger alkali metals. For the purpose of this study, we will assume an identical hydration number of 16 for all structures.

On Fig. 4, we observe that MD-averaged d(001) distances increase with the size of the intercalated cation, matching the trend observed in experimental observations for the sodium and potassium, less so for the larger cations. The description of the GR2 structure proposed in Christiansen *et al.* 2004[18] ($GRNaSO_4$) with 16 water molecules and an alkali cation is therefore a moderately adequate starting point for predicting the interlayer distance of closely related structures.

In conclusion, this study provides a computational comparison between the two descriptions of GR2, with and without intercalated sodium. It shows that only the sodium-intercalated formula ($Fe^{II}_6Fe^{III}_3(OH)_{18}Na(SO_4)_2{\cdot}nH_2O$) with $14 \leq n \leq 16$ can simultaneously match experimental measurements of the interlayer spacing and hydration number. The basal spacing of the hypothetical sodium-free $GRSO_4$ does not match those from the literature without pushing the hydration number well above experimental values.

We demonstrate that the sodium cation has a templating effect on the structure, forming four structured water layers and separating the sulfates into two distinct positions. This templating effect is also evidenced by replacing Na^+ with larger alkali metals (K^+, Rb^+, Cs^+), leading to an increase in c distances that follows the trend in experimental measurements. The resulting water layers are tightly bound to the Na^+, potentially explaining the lack of interlayer swelling of GR2 when compared with other sulfate LDHs. However, demonstrating this templating effect experimentally would require further study of GR2 compounds over larger temperature and humidity ranges than those reported in the literature. Demonstrating a mobility of the intercalated cation, which could not be observed during our short molecular dynamics simulations, may also open up the possibility of using GR2 for simultaneous anionic and cationic exchange. It is also an open question whether this result is generalizable to other types of hydrotalcites, and whether all structures with a similar interlayer distance must necessarily contain sodium.

Conflicts of interest

There are no conflicts to declare.

CRediT author statement

Adam Nelson: Conceptualization, Methodology, Visualization, Investigation, Writing – Original draft. **Christian Ruby**: Writing-Reviewing & Editing. **Erwan André**: Writing – Reviewing & Editing. **Damien Cornu**: Conceptualization, Supervision, Funding acquisition, Writing – Reviewing & Editing.

Acknowledgements

Funding for this study was provided by the CNRS EMERGENCE grants. High Performance Computing resources were partially provided by the EXPLOR center hosted by the University of Lorraine. This work was also granted access to the HPC resources of IDRIS under the allocation *2025-AD010116607* made by GENCI.

Data availability

The output files of the molecular dynamics simulations as well as the Python script used to process the data are freely available *via* DOREL: (OSF link for reviewers before publication) https://osf.io/yqk82/overview?view_only=94a3ec55c4b6453f9865a79406a97862).

Notes and references

1 X. Liang, Y. Zang, Y. Xu, X. Tan, W. Hou, L. Wang and Y. Sun, *Colloids Surf. Physicochem. Eng. Asp.*, 2013, **433**, 122–131.
2 A. R. Sotiles, L. M. Baika, M. T. Grassi and F. Wypych, *J. Am. Chem. Soc.*, 2019, **141**, 531–540.
3 K. K. Sagoe-Crentsil and F. P. Glasser, *Corrosion*, 1993, **49**, 457–463.
4 S. Grousset, F. Kergourlay, D. Neff, E. Foy, J.-L. Gallias, S. Reguer, P. Dillmann and A. Noumowé, *J. Anal. At. Spectrom.*, 2015, **30**, 721–729.
5 Q. Jia, M. Wang, Y. Liu, Y. Gu, X. Wang, T. Yang and L.-Z. Huang, *Water Res.*, 2025, **287**, 124289.
6 N. M. E. Kawas, A. H. Zaki and M. Taha, *RSC Adv.*, 2025, **15**, 18403–18418.
7 Ph. Refait, S. H. Drissi, J. Pytkiewicz and J.-M. R. Génin, *Corros. Sci.*, 1997, **39**, 1699–1710.

8 L. Simon, Ph. Refait and J.-M. R. Génin, *Hyperfine Interact.*, 1998, **112**, 217–222.
9 R. Polly, N. Finck, T. Platte, N. Morelova, F. Heberling, B. Schimmelpfennig and H. Geckeis, *J. Phys. Chem. C*, 2022, **126**, 8016–8028.
10 B. C. Christiansen, T. Balic-Zunic, P.-O. Petit, C. Frandsen, S. Mørup, H. Geckeis, A. Katerinopoulou and S. L. S. Stipp, *Geochim. Cosmochim. Acta*, 2009, **73**, 3579–3592.
11 R. L. Frost, A. W. Musumeci, T. Bostrom, M. O. Adebajo, M. L. Weier and W. Martens, *Thermochim. Acta*, 2005, **429**, 179–187.
12 D. Cornu, R. Coustel, G. Renaudin, G. Rogez, A. Renard, P. Durand, C. Carteret and C. Ruby, *Dalton Trans.*, 2022, **51**, 11787–11796.
13 P. I. R. Moraes, F. Wypych and A. A. Leitão, *J. Phys. Chem. C*, 2019, **123**, 9838–9845.
14 W. Sdiri, R. Coustel, M. Ounacer, D. Cornu, A. Nelson, G. Ona-Nguema, C. Despas, M. Mallet, E. André, C. Truong, W. Nitschke, S. Duval, M. Abdelmoula, L. Bergaoui and C. Ruby, *Surf. Interfaces*, 2026, 108518.
15 L. Simon, M. François, P. Refait, G. Renaudin, M. Lelaurain and J.-M. R. Génin, *Solid State Sci.*, 2003, **5**, 327–334.
16 V. A. Drits, T. N. Sokolova, G. V. Sokolova and V. I. Cherkashin, *Clays Clay Miner.*, 1987, **35**, 401–417.
17 H. C. B. Hansen, O. K. Borggaard and J. Sørensen, *Geochim. Cosmochim. Acta*, 1994, **58**, 2599–2608.
18 B. Christiansen, S. Stipp and T. Balic-Zunic, 2004, pp. A139–A139.
19 B. C. Christiansen, K. Dideriksen, A. Katz, S. Nedel, N. Bovet, H. O. Sørensen, C. Frandsen, C. Gundlach, M. P. Andersson and S. L. S. Stipp, *Inorg. Chem.*, 2014, **53**, 8887–8894.
20 A. Onoguchi, G. Granata, D. Haraguchi, H. Hayashi and C. Tokoro, *R. Soc. Open Sci.*, 2019, **6**, 182147.
21 K. M. N. Alam and E. J. Elzinga, *Environ. Sci. Technol.*, 2023, **57**, 8396–8405.
22 K. B. Ayala-Luis, C. B. Koch and H. C. B. Hansen, *Appl. Clay Sci.*, 2010, **48**, 334–341.
23 C. Bhave and S. Shejwalkar, *Int. J. Environ. Sci. Technol.*, 2018, **15**, 1243–1248.
24 E. Juanmartí i Guiluz, *Treb. Finals Grau TFG - Quím.*
25 J.-P. Jolivet, C. Chanéac and E. Tronc, *Chem. Commun.*, 2004, 481–483.
26 L. Mazeina, A. Navrotsky and D. Dyar, *Geochim. Cosmochim. Acta*, 2008, **72**, 1143–1153.
27 J.-M. R. Génin, A. A. Olowe, Ph. Refait and L. Simon, *Corros. Sci.*, 1996, **38**, 1751–1762.
28 M. A. Cooper and F. C. Hawthorne, *Can. Mineral.*, 1996, **34**, 91–97.
29 P. Hohenberg and W. Kohn, *Phys. Rev.*, 1964, **136**, B864–B871.
30 W. Kohn and L. J. Sham, *Phys. Rev.*, 1965, **140**, A1133–A1138.
31 G. Kresse and J. Hafner, *Phys. Rev. B*, 1993, **47**, 558–561.
32 G. Kresse and J. Hafner, *Phys. Rev. B*, 1993, **48**, 13115–13118.
33 G. Kresse and J. Furthmüller, *Phys. Rev. B*, 1996, **54**, 11169–11186.
34 J. P. Perdew, K. Burke and M. Ernzerhof, *Phys. Rev. Lett.*, 1996, **77**, 3865–3868.
35 D. G. Costa, A. B. Rocha, R. Diniz, W. F. Souza, S. S. X. Chiaro and A. A. Leitão, *J. Phys. Chem. C*, 2010, **114**, 14133–14140.
36 G. Pérez-Sánchez, T. L. P. Galvão, J. Tedim and J. R. B. Gomes, *Appl. Clay Sci.*, 2018, **163**, 164–177.
37 V. I. Anisimov, J. Zaanen and O. K. Andersen, *Phys. Rev. B*, 1991, **44**, 943–954.
38 M. Cococcioni and N. Marzari, *Phys. Rev. Mater.*, 2019, **3**, 033801.
39 A. Tkatchenko and M. Scheffler, *Phys. Rev. Lett.*, 2009, **102**, 073005.
40 H. J. Monkhorst and J. D. Pack, *Phys. Rev. B*, 1976, **13**, 5188–5192.
41 M. Parrinello and A. Rahman, *Phys. Rev. Lett.*, 1980, **45**, 1196–1199.
42 W. G. Hoover, A. J. C. Ladd and B. Moran, *Phys. Rev. Lett.*, 1982, **48**, 1818–1820.
43 C. R. Harris, K. J. Millman, S. J. Van der Walt, R. Gommers, P. Virtanen, D. Cournapeau, E. Wieser, J. Taylor, S. Berg, N. J. Smith, R. Kern, M. Picus, S. Hoyer, M. H. van Kerkwijk, M. Brett, A. Haldane, J. F. del Río, M. Wiebe, P. Peterson, P. Gérard-Marchant, K. Sheppard, T. Reddy, W. Weckesser, H. Abbasi, C. Gohlke and T. E. Oliphant, *Nature*, 2020, **585**, 357–362.
44 J. D. Hunter, *Comput. Sci. Eng.*, 2007, **9**, 90–95.
45 X. Hou, D. L. Bish, S.-L. Wang, C. T. Johnston and R. J. Kirkpatrick, *Am. Mineral.*, 2003, **88**, 167–179.
46 R. Caminiti, G. Licheri, G. Paschina, G. Piccaluga and G. Pinna, *J. Chem. Phys.*, 1980, **72**, 4522–4528.

View Article Online
DOI: 10.1039/D6CP00496B

View Article Online
DOI: 10.1039/D6CP00496B

Data for this article are available at OSF at
https://osf.io/yqk82/overview?view_only=94a3ec55c4b6453f9865a79406a97862.

This is a reviewer link. If accepted, a new link will be available on university database DOREL.